Supplementary information

The sirtuin SIRT6 blocks IGF-Akt signaling and development of cardiac hypertrophy by targeting c-Jun.

Nagalingam R. Sundaresan[1], Prabhakaran Vasudevan[2], Lei Zhong[3], Gene Kim[4], Sadhana Samant[1], Vishwas Parekh[2], Vinodkumar B. Pillai[1], PV Ravindra[1], Madhu Gupta[5], Valluvan Jeevananadam[1], John M. Cunningham[2], Chu-Xia Deng[6], David B. Lombard[7], Raul Mostoslavsky[3] and Mahesh P. Gupta[1],*

[1]Department of Surgery, Committee on Cellular and Molecular Physiology, University of Chicago, Chicago, IL.

[2]Department of Pediatrics, Committee on Developmental Biology, University of Chicago, Chicago, IL.

[3]The Massachusetts General Hospital Cancer Center, Harvard Medical School, Boston MA,

[4]Department of Medicine, Section of Cardiology, University of Chicago, Chicago, IL.

[5]Department of Physiology and Biophysics, University of Illinois at Chicago, Chicago, IL.

[6]National Institute of Diabetes, Digestive and Kidney Diseases, US, National Institutes of Health, Bethesda, MD.

[7]Department of Pathology and Institute of Gerontology, University of Michigan, Ann Arbor, MI.

*Address of corresponding author: Department of Surgery, MC 5040, University of Chicago, 5841 S. Maryland Avenue, Chicago, IL 60637**:** **mgupta@surgery.bsd.uchicago.edu**

Supplementary Figure 1

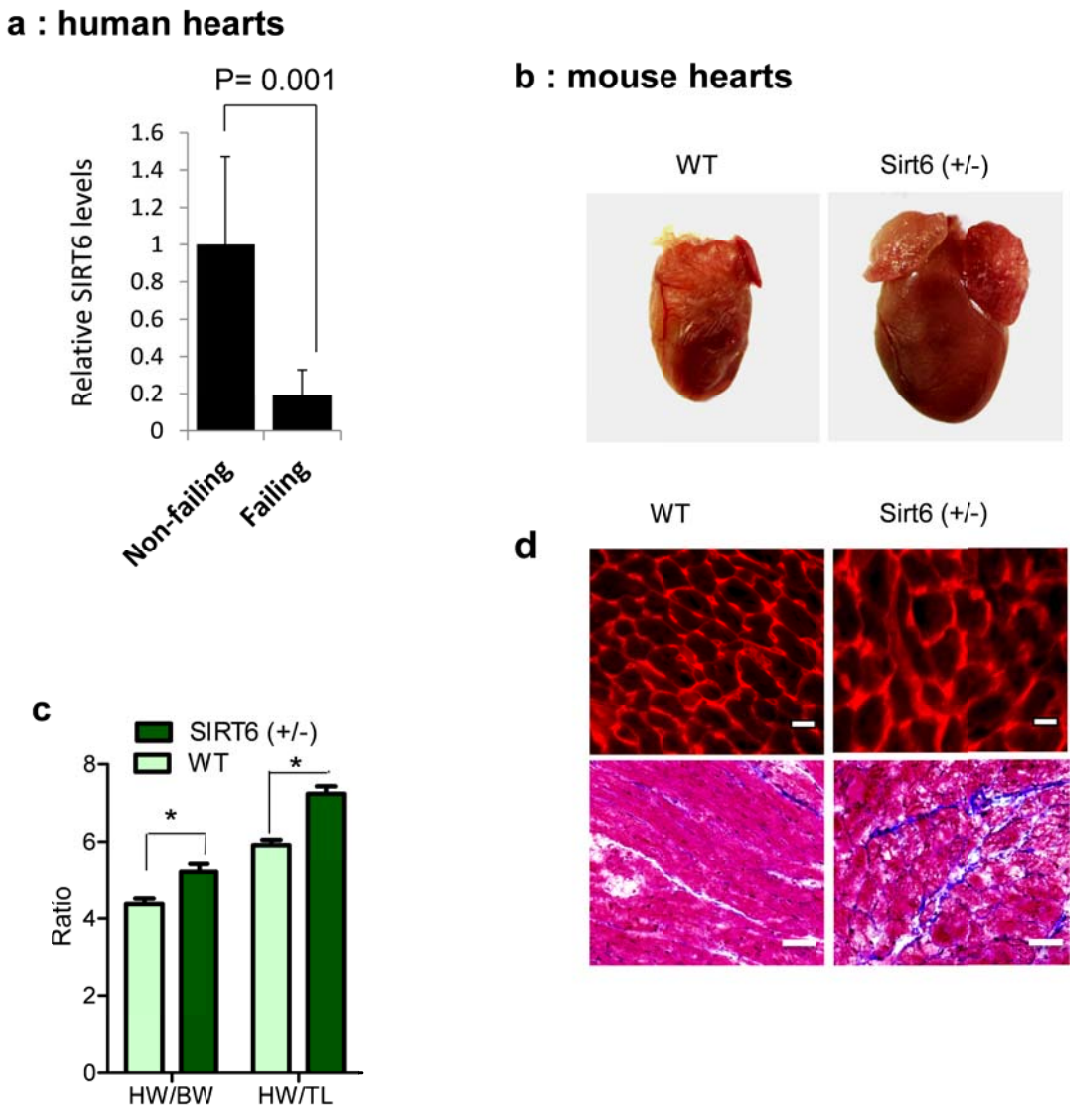

Supplementary figure 1: Reduced SIRT6 levels lead to induction of cardiac hypertrophy. **(a)** Quantification of SIRT6 levels in non-failing and failing human hearts (for details see supplementary table1). **(b)** Hypertrophy of SIRT6 (+/-) hearts, compared to WT control at 6 months of age. **(c)** HW/BW and HW/TL ratios in WT and SIRT6 (+/-) mice. **(d)** Heart sections showing increased cardiomyocyte size (scale bar 10μM) and fibrosis (bar 40μM) in SIRT6 (+/-) hearts compared to WT controls.

Supplementary Figure 2

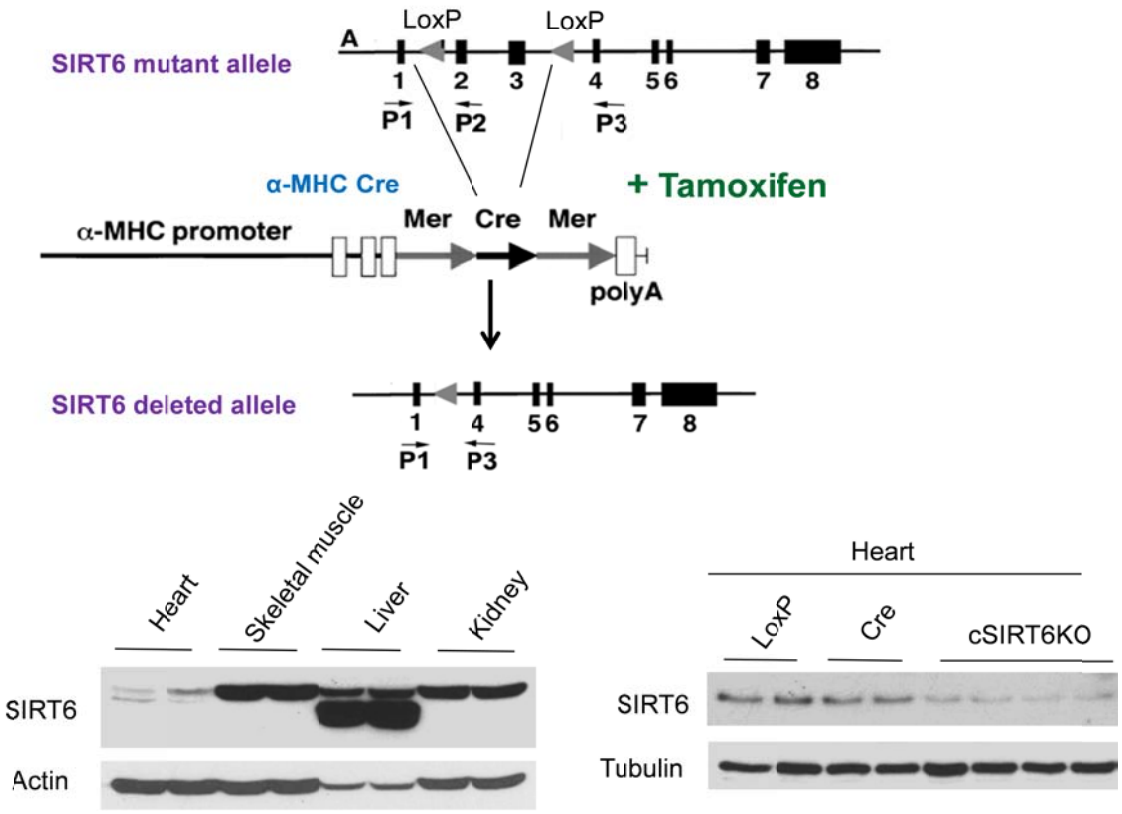

Supplementary figure 2: Generation of inducible cardiac specific SIRT6 knockout mice. Mice carrying both *loxp/loxp* and *α-MHC-Cre* alleles were injected with tamoxifen at 4 weeks of age for three consecutive days. SIRT6 deletion was determined by western blotting of different tissue lysates.

Supplementary Figure 3

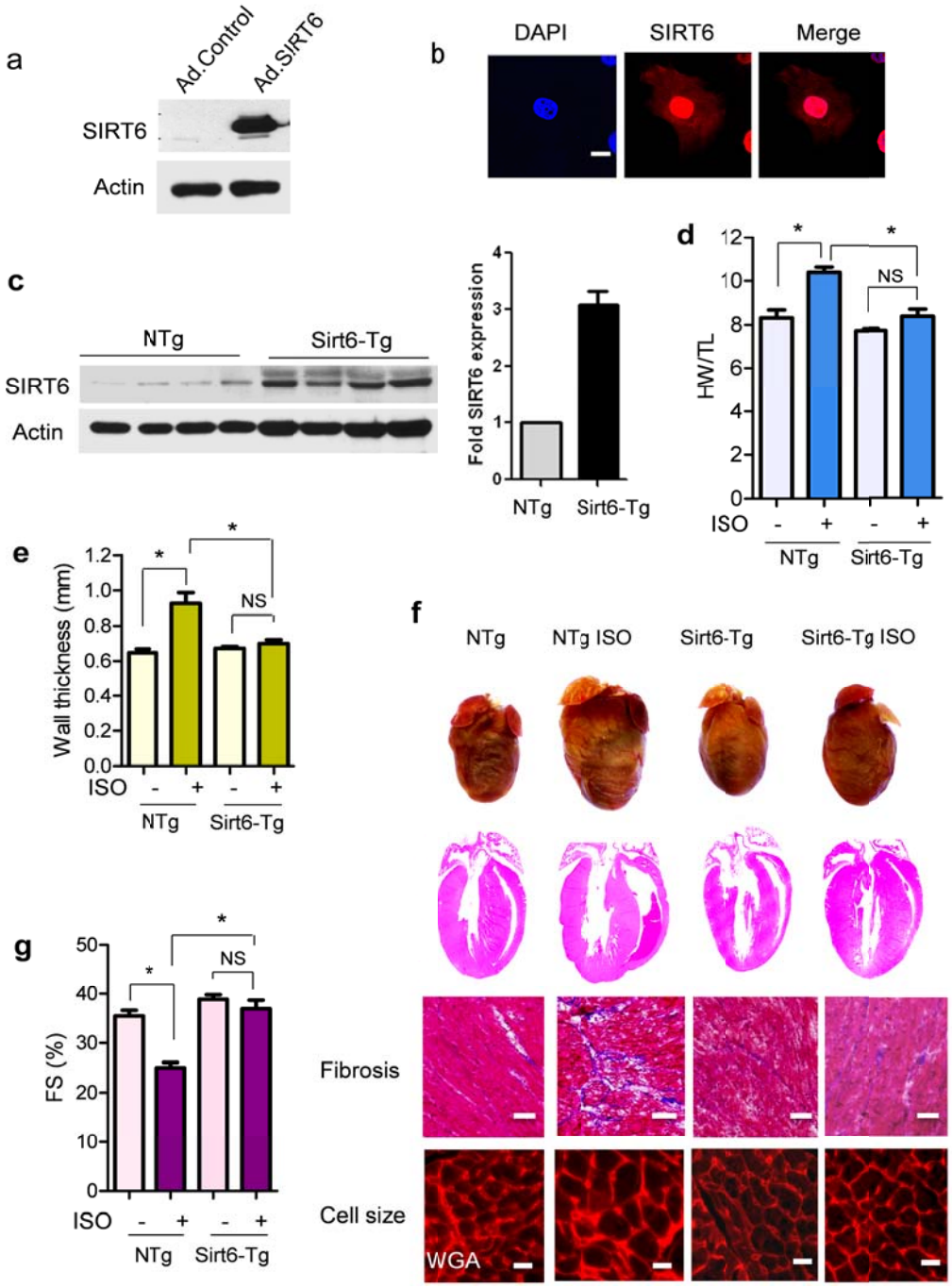

Supplementary figure 3: SIRT6 over expression blocks agonist-mediated cardiac hypertrophy. **(a)** Western blots showing expression of SIRT6 adenovirus in cardiomyocytes. **(b)** Nuclear localization of SIRT6 in cardiomyocytes (scale bar 10μM). (**c**) Expression levels of SIRT6 in non-transgenic (NTg) control and SIRT6.Tg hearts. Mean ± SD, n=4. (**d**) N.Tg and SIRT6-Tg mice were treated with vehicle or isoproterenol (ISO, 8.7 mg/kg/d for 7 days), and their HW/TL ratio was determined; mean ± SD, n =5-6. (**e**) Left ventricular wall thickness as determined by echocardiography. Mean ± SD, n = 5-6. (**f**) Representative whole hearts and heart sections of N.Tg and SIRT6-Tg mice subjected to develop ISO-mediated hypertrophy. Scale bar to detect fibrosis 40μM, and for cell size 10μM. WGA indicates wheat germ agglutinin. (**g**) Fractional shortening of same mice as in panel e. Mean ± SD, n = 5-6. *p<0.001.

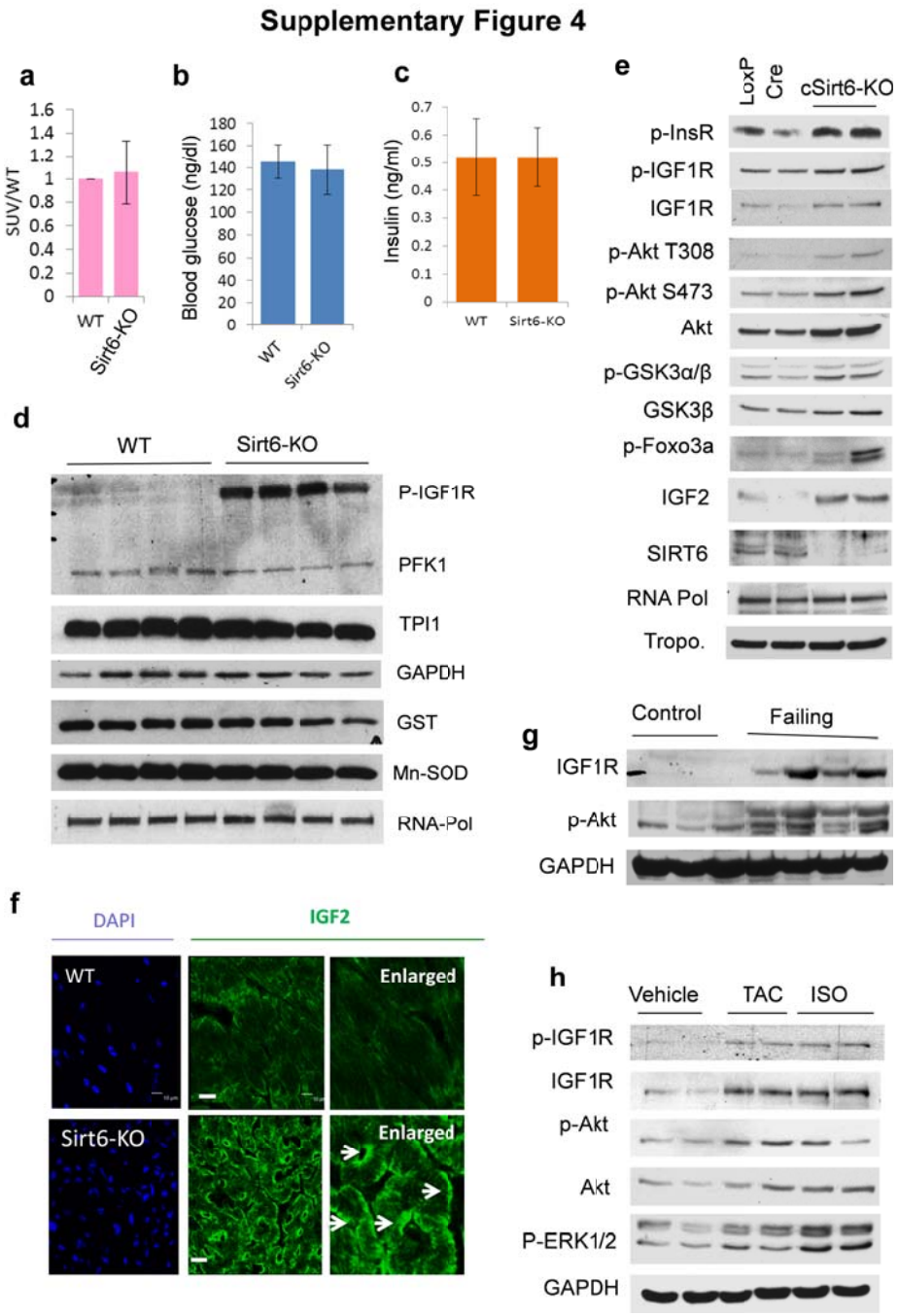

Supplementary figure 4: Biochemical characteristics of SIRT6-deficent hearts. (a) Standard uptake value (SUV) ratio of labeled ^{18}FDG-Glucose incorporation in the heart of WT and SIRT6-KO mice, n = 3. **(b)** Blood glucose levels in WT and SIRT6KO mice at 3 months of age. **(c)** Serum insulin levels of the WT and SIRT6KO mice at 3 months of age, n = 10-12. **(d)** Western analysis of Hif-1α target glycolytic genes and NF-kB target antioxidant genes. Phospho-IGF1R is used as positive control. **(e)** Western analysis of IGF signaling related genes in controls and cardiac-specific SIRT6KO (cSIRT6KO) heart lysates. **(f)** Confocal images showing membrane localization of IGF2 (green) in WT and SIRT6KO hearts (scale bar 10μM). Arrows indicate membrane bound IGF2 in myocytes. **(g)** Western analysis of control and failing human heart lysates. **(h)** Western analysis of IGF/Akt signaling related targets in control and hypertrophied mouse heart lysates. Cardiac hypertrophy was induced by pressure overload (TAC) or isoproterenol (ISO) infusion in mice.

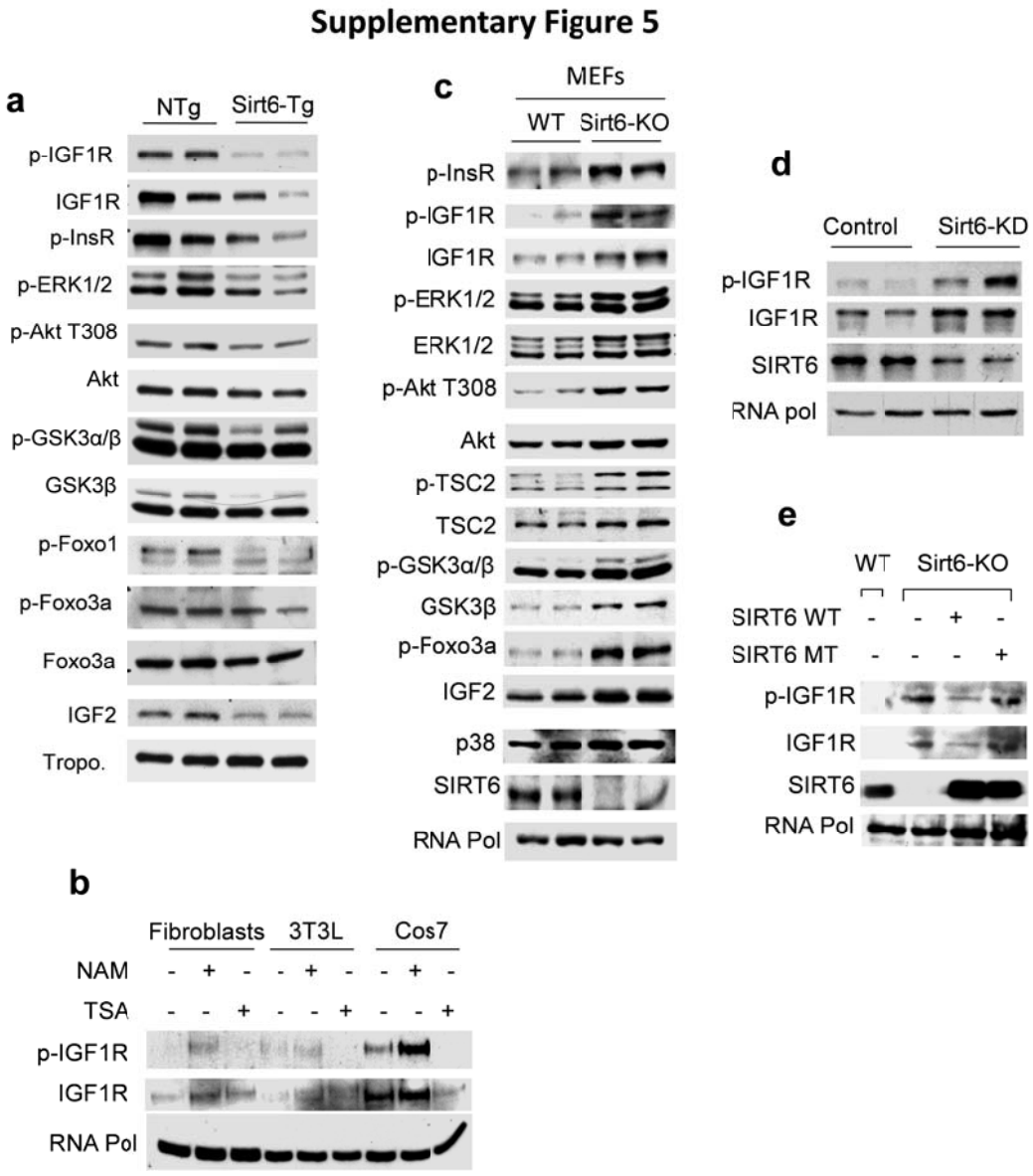

Supplementary figure 5: Western analysis of IGF signaling related genes. (a) Expression levels of IGF signaling related genes in NTg and SIRT6-Tg hearts. **(b)** Expression and phosphorylation of IGF1R in vehicle, nicotinamide (NAM) and trichostatin-A (TSA) treated cells. **(c)** Increased expression and phosphorylation of IGF signaling related genes in WT and SIRT6-KO MEFs. **(d)** IGF1R levels in control and SIRT6-KD 293T cells. **(e)** Over expression of WT, but not the mutant (MT) SIRT6 suppressed the IGF1R signaling in SIRT6-KO fibroblasts.

Nature Medicine: doi:10.1038/nm.2961

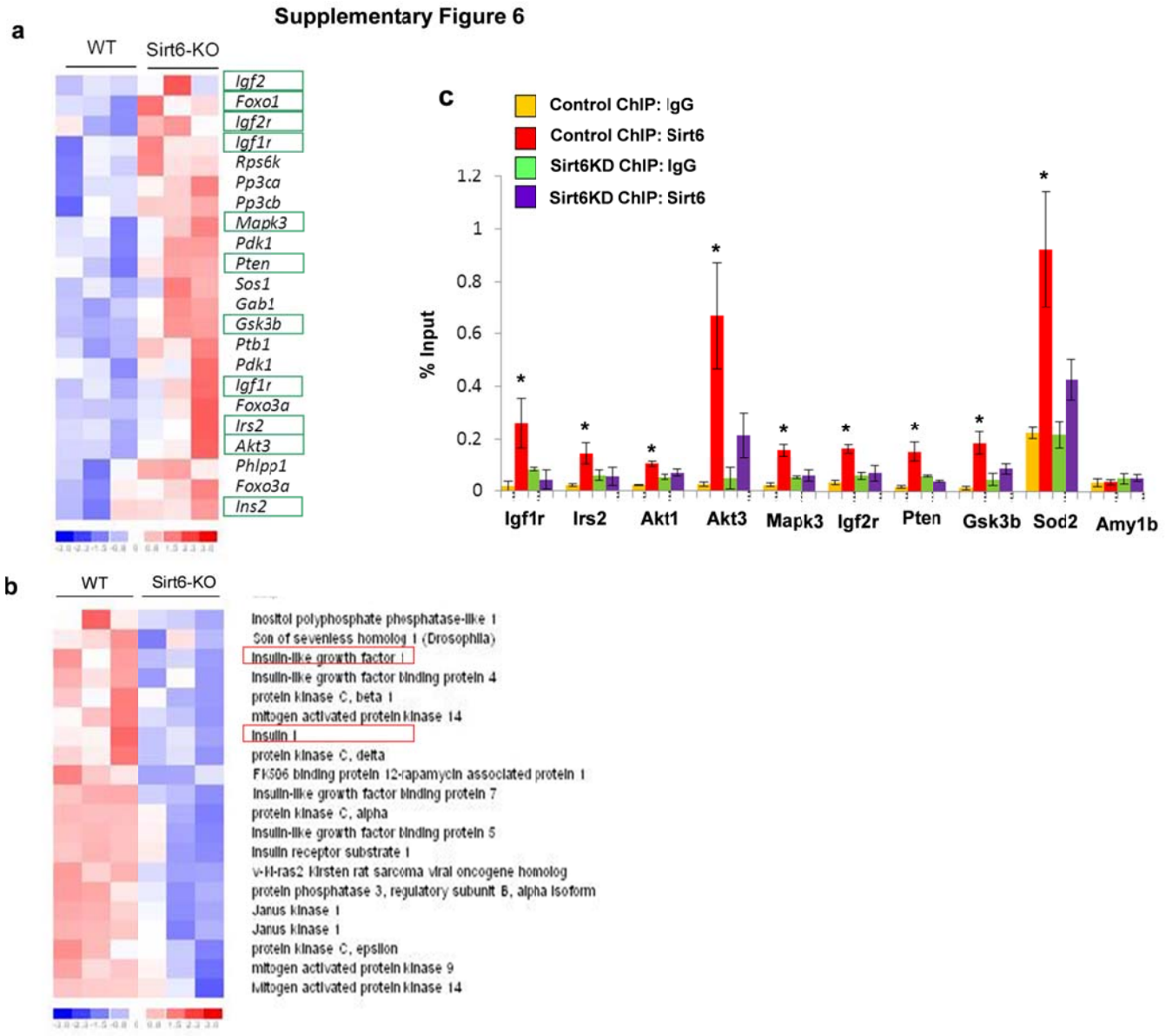

Supplementary figure 6: SIRT6-dependent regulation of IGF signaling related genes. **(a and b)** Comparative microarray analysis of IGF signaling related genes in wild type and SIRT6-KO skeletal muscle samples. **(c)** The ChIP analysis data from Fig. 4e is shown without normalization as % input.

Supplementary Figure 7

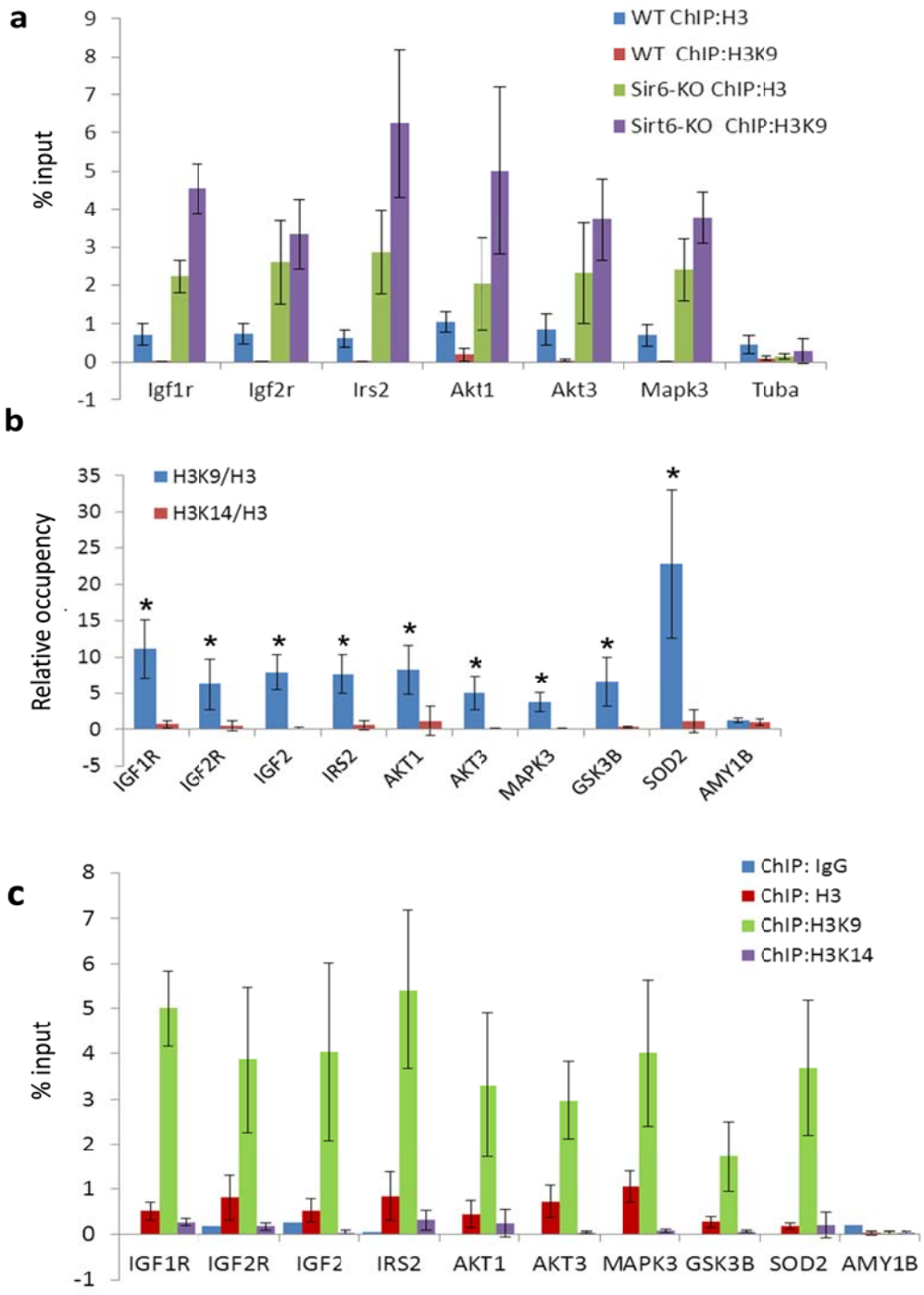

Supplementary figure 7: The ChIP analysis with wild-type and SIRT6 knockout hearts and cells. (a) The ChIP analysis was performed in WT and SIRT6-KO heart samples with use of Ac-H3K9 (H3K9) and H3 antibodies. Acetylation of H3K9 at promoters is shown relative to total H3 levels and the data is shown as % input. **(b and c)** ChIP analysis was performed with use of Ac-H3K9, Ac-H3K14 and H3 antibodies in SIRT6-KD stable 293T cells. The data presented as either normalized with H3 levels (b) or shown without normalization as % input (c).

Supplementary Figure 8

Nature Medicine: doi:10.1038/nm.2961

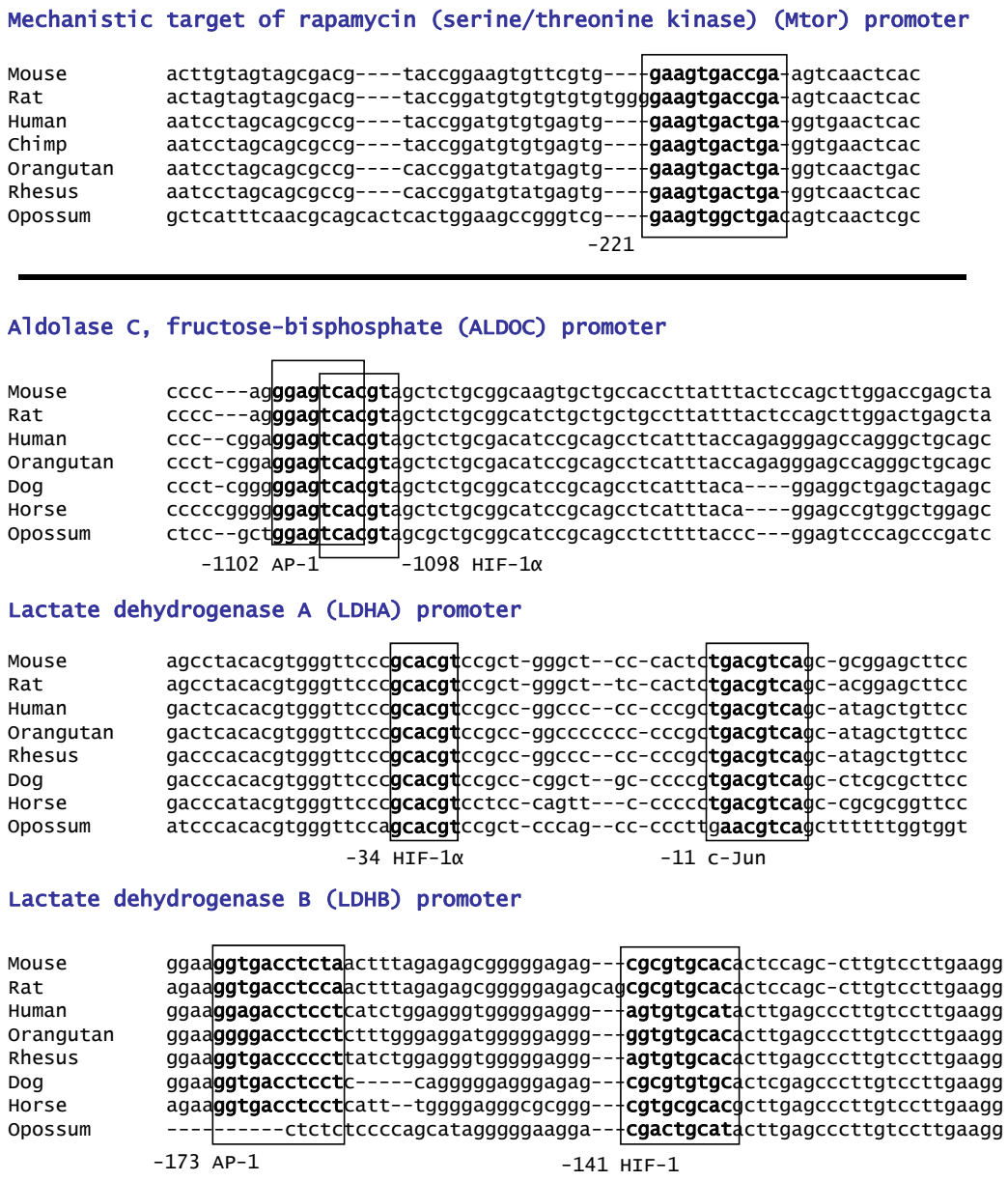

Supplementary figure 8: In-silico analysis of evolutionarily conserved c-Jun binding sites in the promoters of different genes. The transcription factor binding site analysis was done using TRANSFAC software (Biobase GmbH); evolutionary conservation analysis was carried out using UCSC Genome Browser. Nucleotide sequences in bold denote AP-1/c-Jun consensus binding sites, and number below denotes distance (bp) from the transcription start site of the respective mouse gene. Upon extensive analysis, we confirmed that InsR does not have any conserved binding site for AP1/c-Jun, though it showed increased expression in SIRT6KO hearts. Interestingly, our in silico analysis does not find any c-Jun binding sites in HIF-1α target glycolytic genes, PFK1, TPI1, PDK1 and GAPDH. However, few glycolytic genes especially ALDOC, LDHA, and LDHB have both c-Jun and HIF-1α binding sites very close to their proximal promoter regions.

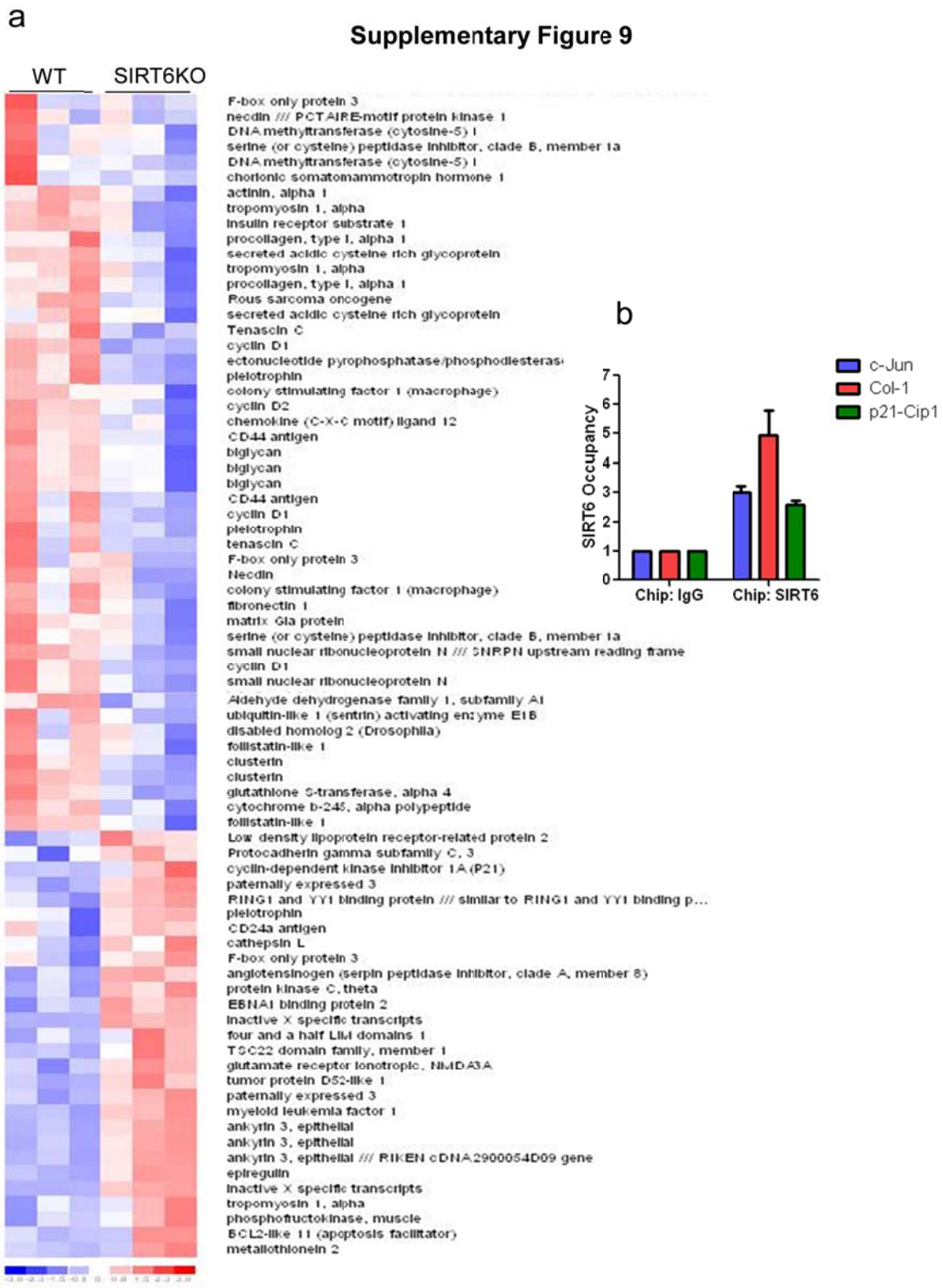

Supplementary figure 9: Analysis of AP1 target genes. (a) Comparative microarray analysis of AP-1 target genes in wild type and SIRT6-KO skeletal muscle samples. **(b)** ChIP analysis showing SIRT6 binding to AP1 target gene promoters. Mean ± SD, n = 3.

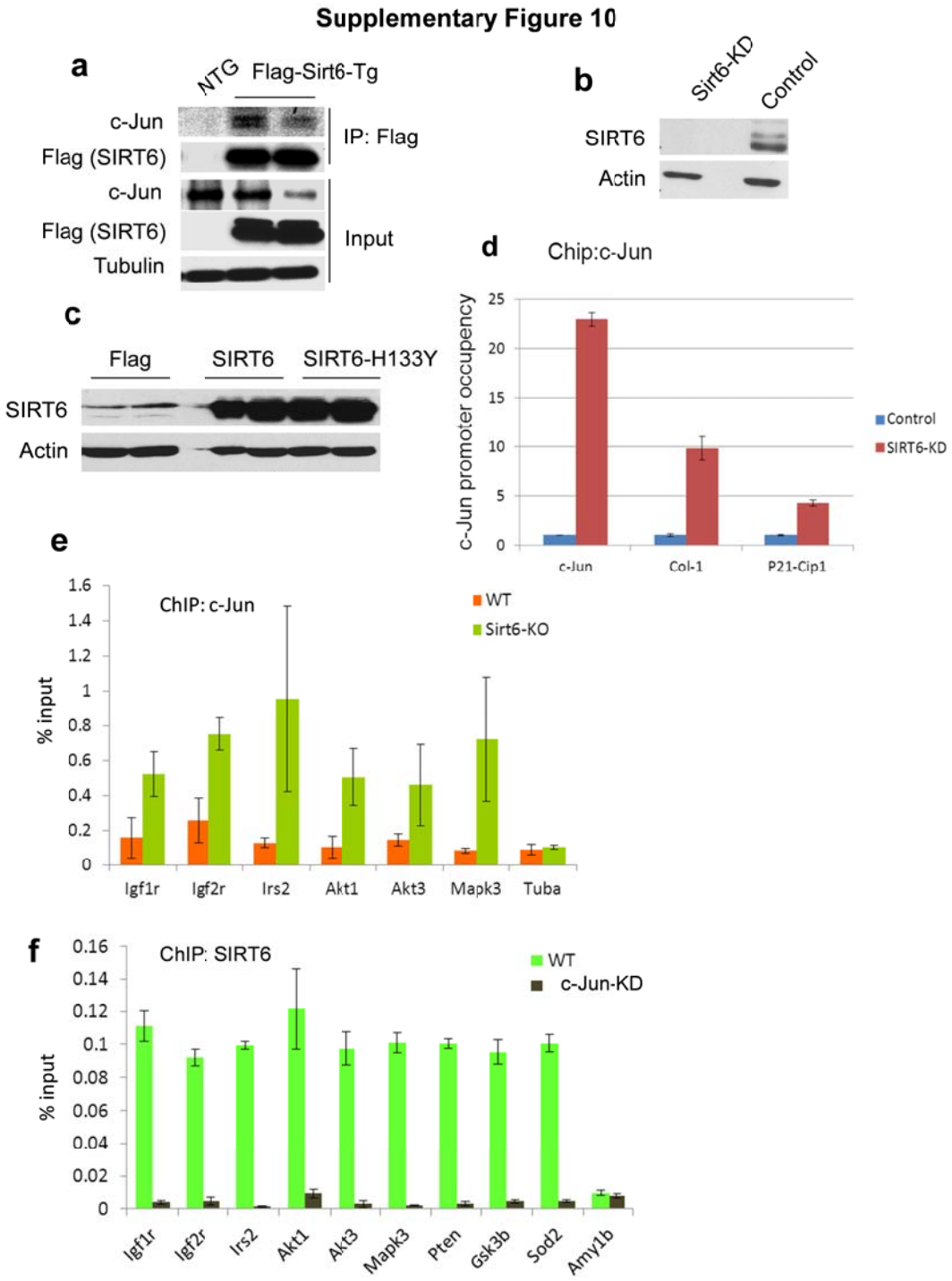

Supplementary figure 10: SIRT6 associates with c-Jun on IGF signaling related genes. (a) SIRT6 was immunoprecipitated from the SIRT6 transgenic mouse hearts using Flag-tag specific antibody. The interaction of SIRT6 with c-Jun was determined by western blotting. **(b and c)** SIRT6 levels in SIRT6KD (b) and overexpressing (c) cells determined by western blotting. **(d)** The ChIP analysis of c-Jun occupancy in the promoters of IGF signaling related genes of control and SIRT6-KD stable 293T cells. **(e)** The ChIP analysis data from Fig. 5e is presented without normalization as % input. **(f)** The ChIP analysis data from Fig. 5f is shown without normalization as % input.

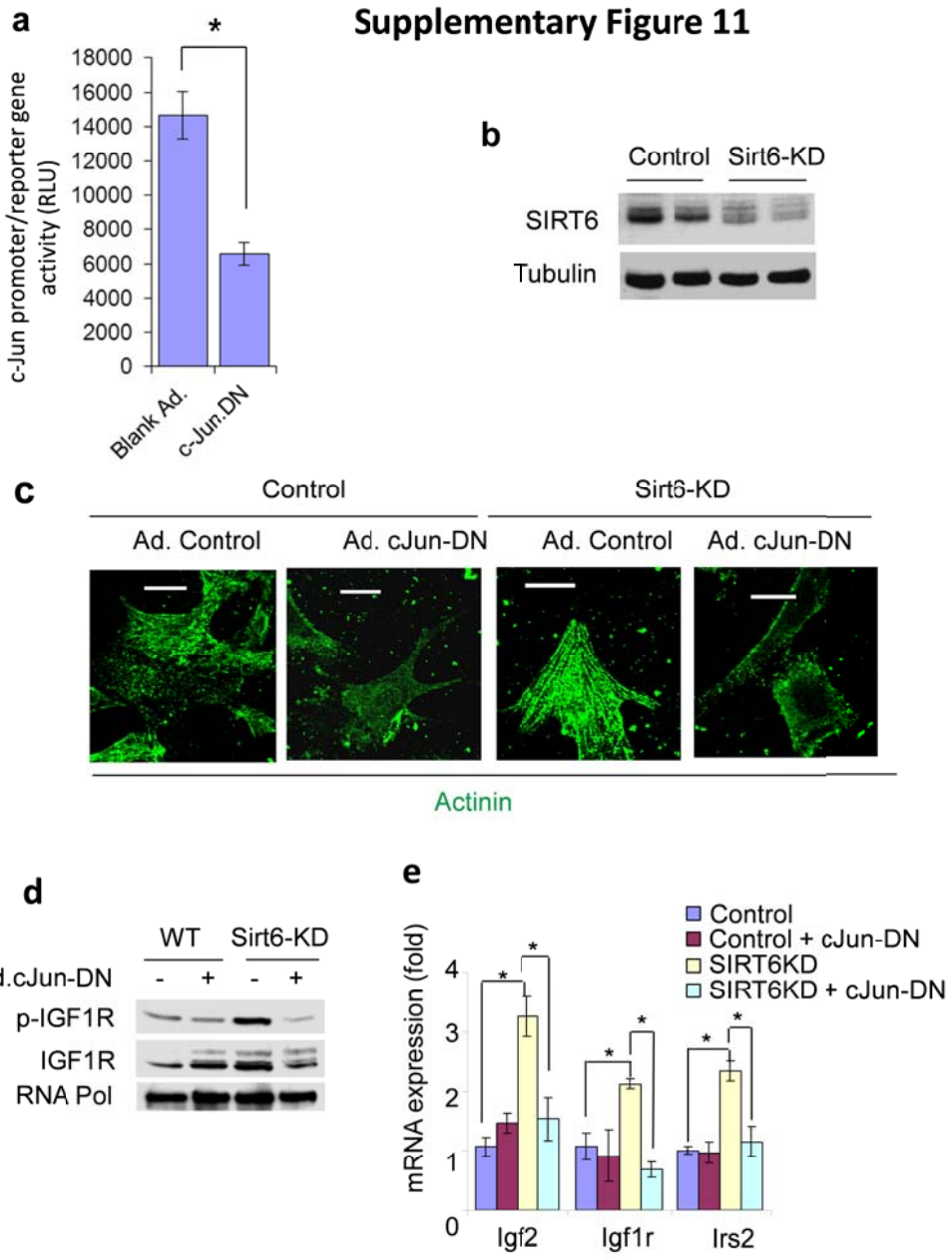

Supplementary figure 11: c-Jun inhibition blocks hypertrophy of SIRT6-KD cardiomyocytes. **(a)** A promoter/ reporter assay showing that adenovirus vector expressing dominant negative (DN) form of c-Jun inhibits activity of endogenous c-Jun. **(b)** Western blots showing SIRT6 knockdown in neonatal rat cardiomyocytes by use of lentiviral vectors (Open Biosystem). **(c)** Confocal imaging of control and SIRT6KD cardiomyocytes over expressed with dominant-negative (DN) form of c-Jun and stained for actinin to visualize sarcomere organization (scale bar 20μM). **(d)** Western blot analysis of IGF1R expression and phosphorylation in WT and SIRT6-KD cardiomyocytes infected with control or c-Jun-DN adenovirus. **(e)** Real-time PCR analysis of representative IGF2 signaling related genes in WT and SIRT6-KD cardiomyocytes infected with control or c-Jun-DN adenovirus. Mean ± SD, n=3-5, *p<0.001.

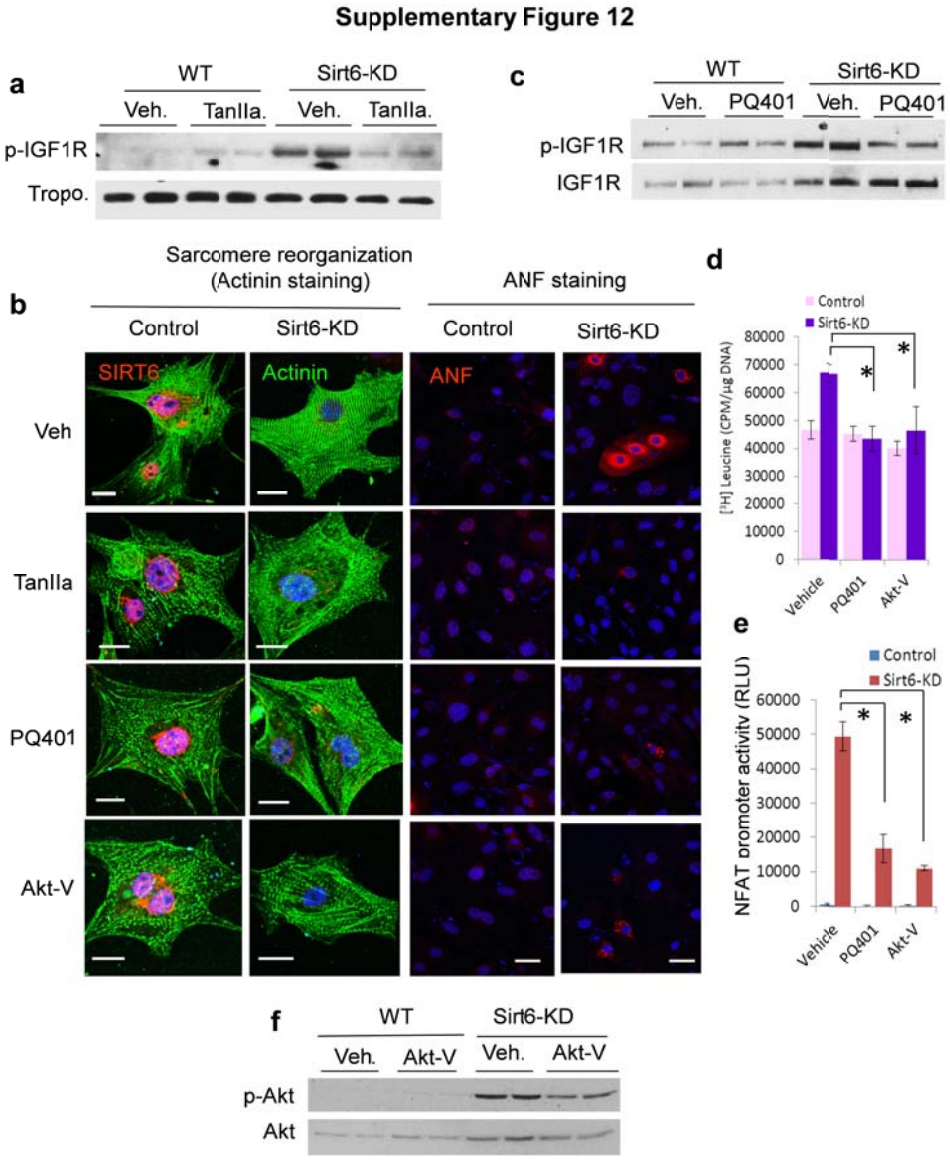

Supplementary figure 12: AP1 and IGF-Akt signaling inhibitors block hypertrophy of SIRT6-deficent cardiomyocytes in vitro. (a) Western analysis of IGF1R phosphorylation in WT and SIRT6KD neonatal rat cardiomyocytes treated with vehicle or Tan-IIa. **(b)** Sarcomere organization and ANF expression in cardiomyocytes treated with different inhibitors. Sarcomeric organization was determined by staining cells for sarcomeric α-actinin (green) and SIRT6 (red) (Scale bar 20µM). ANF release (red) was determined by staining cells with an anti-ANF antibody. DAPI stain was used to mark position of nuclei (Scale bar 50µM). **(c)** Western analysis of IGF1R phosphorylation in cardiomyocytes treated with vehicle or the inhibitor, PQ401 **(d)** Control and SIRT6KD cardiomyocytes were treated with vehicle, PQ401 (10 µM) or Akt-V (0.5µM) for 48 hours. Incorporation of [^{3}H]-leucine into cellular protein was determined and normalized to DNA content of cells. **(e)** Cardiomyocytes were infected with control and NFAT-luciferase promoter/reporter expressing adenovirus vector and treated with vehicle, PQ401 (10 µM) or Akt-v (0.5µM). Cell extracts were analyzed for luciferase activity after 24 hours. Mean ± SD, n = 5-8, *P< 0.001. **(f)** Western analysis of Akt expression and phosphorylation in WT and SIRT6KD cardiomyocytes treated with vehicle or Akt-v inhibitor.

Supplementary Figure 13

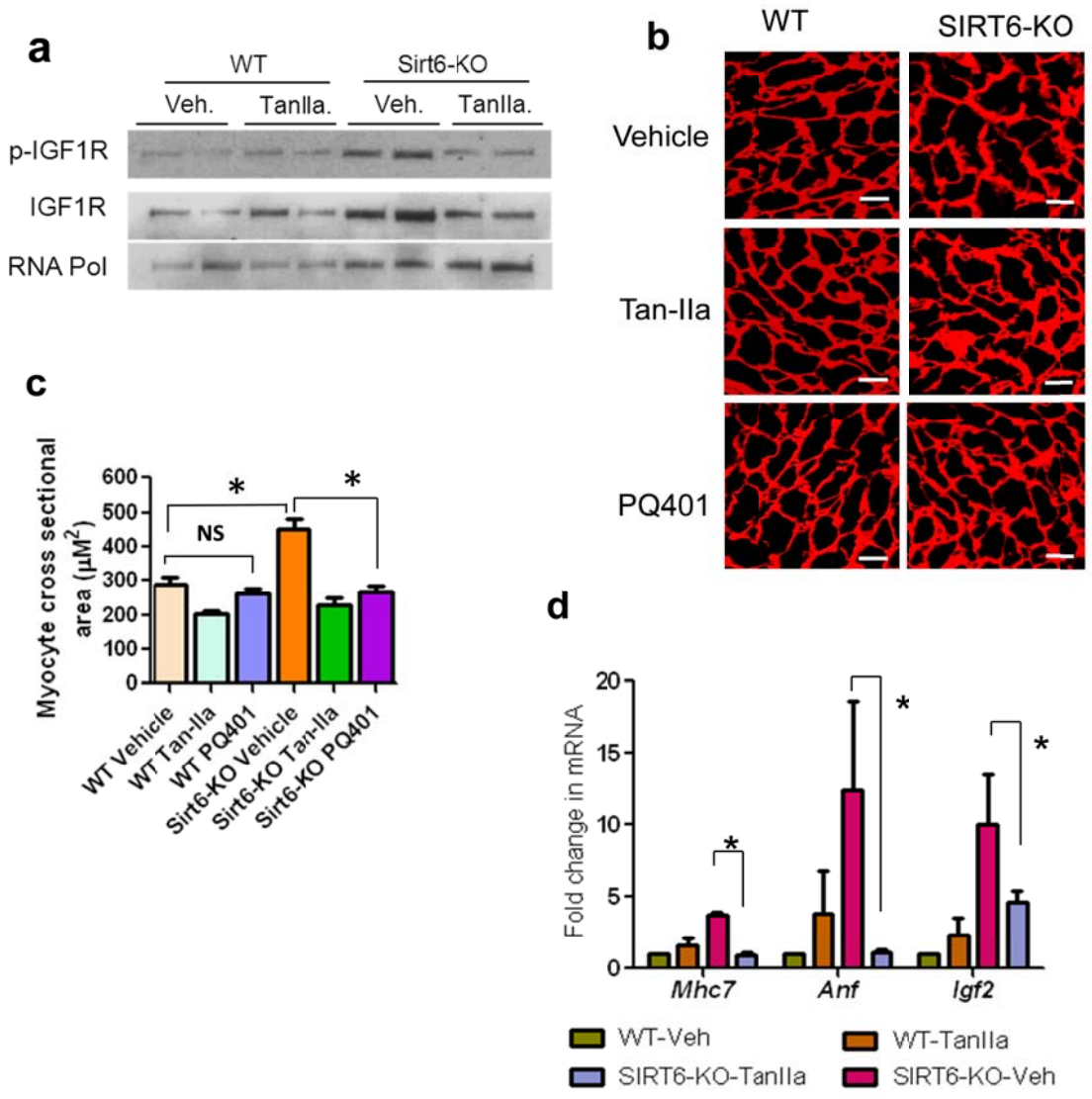

Supplementary figure 13: AP1 and IGFR inhibitors block hypertrophy of SIRT6KO hearts. **(a)** Western analysis of IGF1R expression and phosphorylation in heart lysates of WT and SIRT6-KO mice treated with vehicle or Tan-IIa. **(b and c)** Cardiomyocyte cross sectional area in WT and SIRT6KO mice injected with vehicle or AP1 inhibitor, Tan-IIa (1 mg/kg/day) or IGF1R inhibitor, PQ401 (1 mg/kg/day) for two weeks. Mean ±SD, n= 6 (scale bar 10μM). **(d)** Real-time PCR analysis of cardiac fetal genes (Mhc7 and Anf) and Igf2 gene expression in WT and SIRT6-KO mice injected with vehicle or Tan-IIA. (mean ± SD, n=4-5 mice, *p<0.001).

Supplementary Figure 14

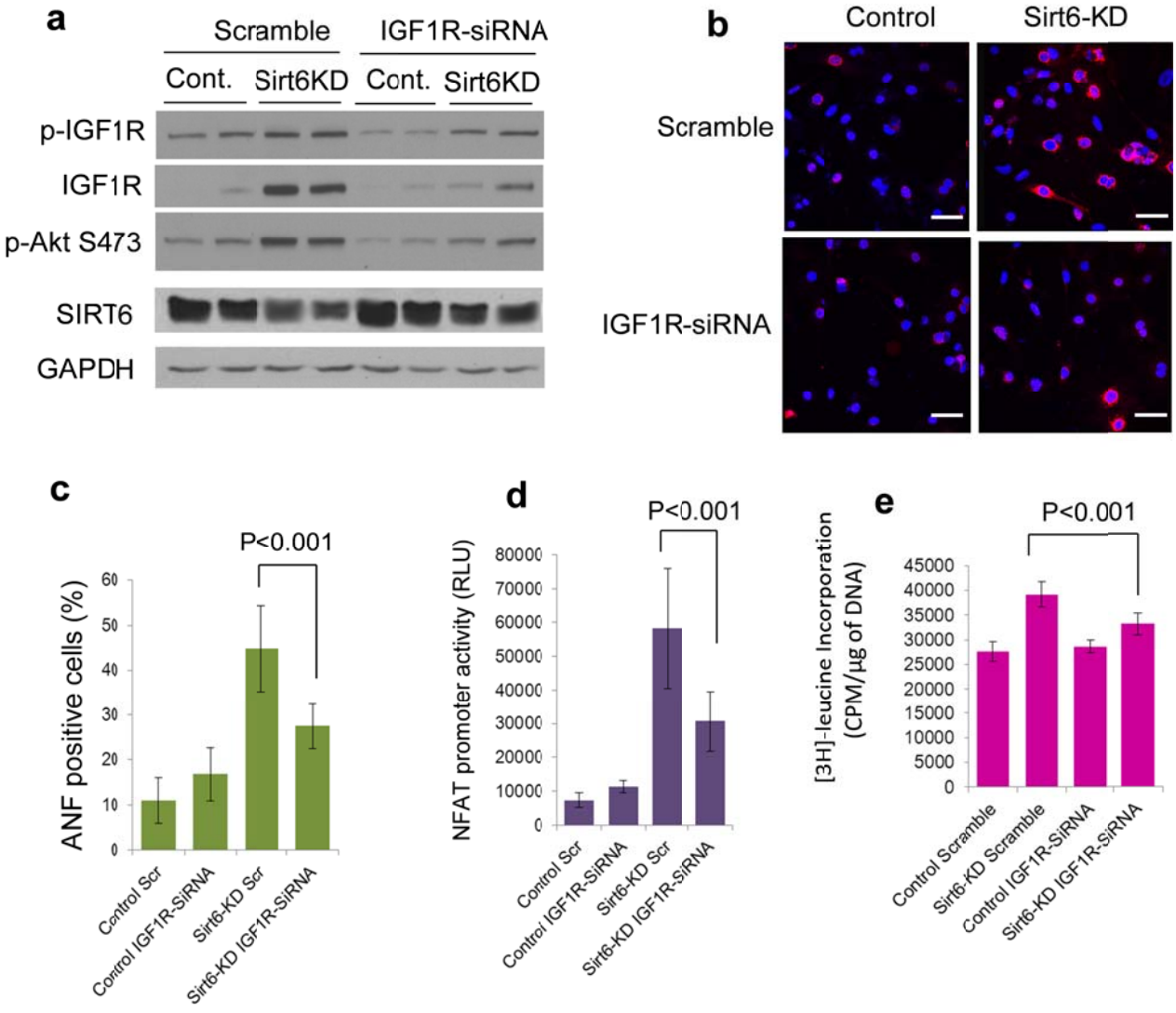

Supplementary figure 14: IFG1R knockdown blocks hypertrophy of SIRT6-KD cardiomyocytes. (a) Western analysis showing IGF1R knockdown in control and SIRT6-deficient (SIRT6KD) cardiomyocytes by use of siRNA. **(b to e)** IGF1R knockdown blocks hypertrophic response of SIRT6-deficient cardiomyocytes, as measured by ANF release from nuclei (b and c), NFAT promoter/reporter activity (d), and ^{3}H-Leucine incorporation into cellular proteins (e). Values are mean ±SD, n= 4-8. Scr indicates scrambled siRNA. Panel b scale bar 50µM.

Supplementary Figure 15

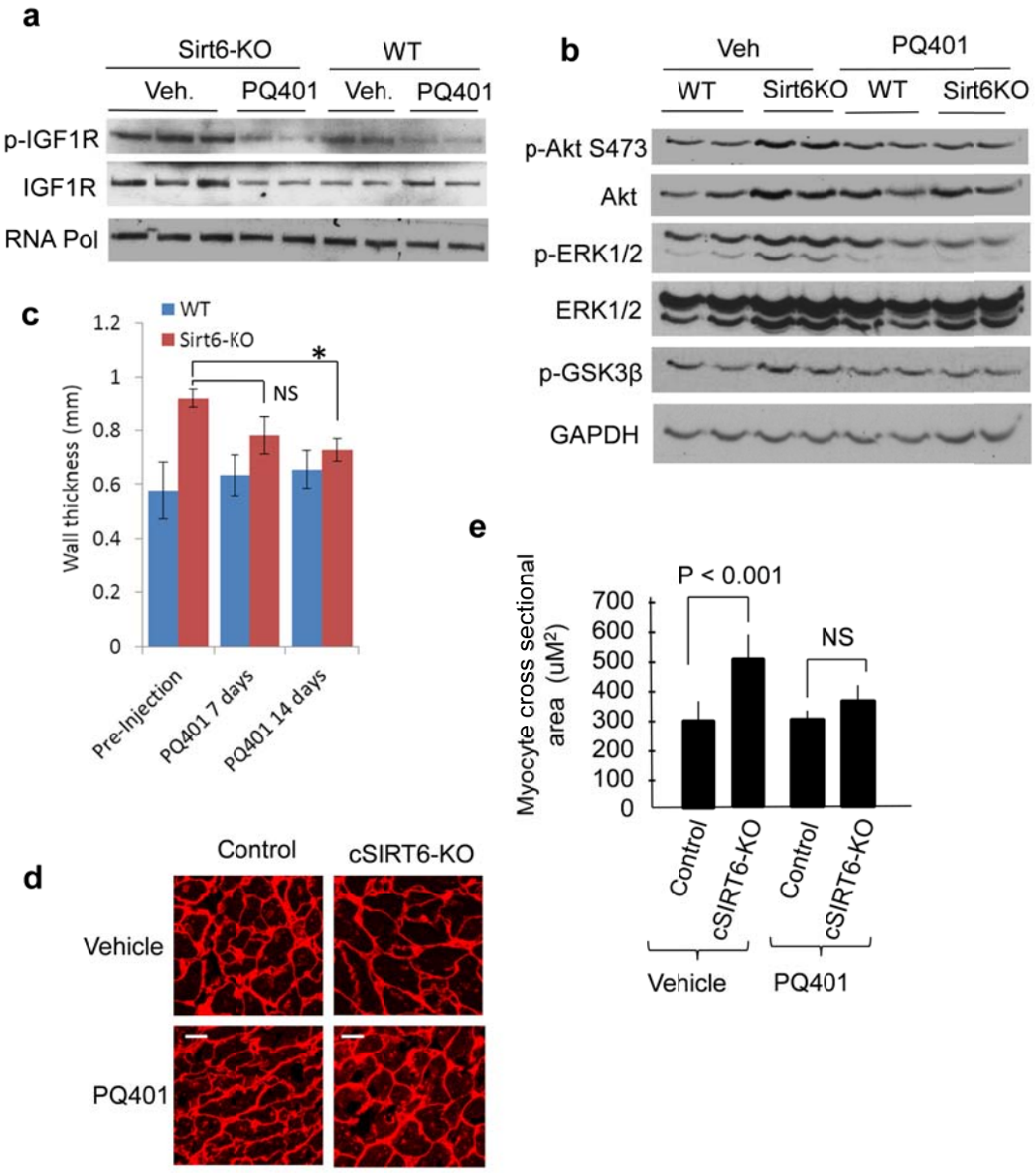

Supplementary figure 15: IGF1R inhibitor, PQ401 blocks cardiac hypertrophy of SIRT6KO mice. (a and b) Western analysis of the heart lysate of wild-type and SIRT6-KO mice treated with vehicle or PQ401 (1 mg/kg/day) for two weeks. **(c)** Analysis of left ventricular wall thickness in WT and SIRT6KO mice injected with vehicle or IGF1R inhibitor, PQ401 for indicated time periods. Mean ± SD, n=4-5, *p<0.001. **(d and e)** Cardiomyocyte cross sectional area in the WT and cardiac-specific SIRT6-KO (cSIRT6KO) mice injected with vehicle or PQ401 for two weeks. Mean ±SD, n= 6-8. Panel d scale bar 10μM.

Supplementary table 1: Clinical characteristics of patients and their corresponding cardiac SIRT6 levels.

						Medical Treatments				
Patients	**Age**	**Gender**	**Diagnosis**	**Dgn**	**Dbt**	**β-Blk**	**ACEI**	**Diuretics**	**Ca-Blx**	**SIRT6**
Non-failing hearts										
NF1	48	M	MVD	--	--	+	--	+	--	1
NF2	39	F	MVD	--	--	+	--	+	--	1.85
NF3	65	M	MVD	--	--	--	--	+	--	1.5
NF4	50	M	Donor dysfunction	--	--	--	--	--	--	2.4
NF5	76	M	MVD	--	--	--	+	+	--	1.6
NF6	7	F	VSD	--	--	--	--	--	--	0.7
NF7	45	M	Donor dysfunction	--	--	--	--	--	--	0.7
NF8	38	M	Donor dysfunction	--	--	--	--	--	--	0.8
Failing hearts										
F-1	57	M	IsCMP	NA	NA	NA	NA	NA	NA	0.1
F-2	56	M	IdCMP	--	+	+	--	+	--	0.15
F-3	65	F	DCM	--	--	+	+	--	--	0.25
F-4	55	M	IsCMP	--	--	+	--	+	--	0.1
F-5	59	M	IsCMP	--	--	+	--	--	--	0.2
F-6	53	F	IdCMP	--	--	+	+	--	--	0.15
F-7	53	M	IsCMP	--	--	+	+	--	--	0.3
F-8	66	M	DCM	--	--	+	+	+	--	0.35
F-9	43	F	DCM	--	--	+	+	+	--	0.4
F-10	82	M	DCM	+	--	+		+	--	0.3
F-11	13	M	IdCMP	NA	NA	NA	NA	NA	NA	0.8
F-12	26	M	DCM	--	+	--	--	--	--	0.15
F-13	61	F	IsCMP	--	--	--	--	--	--	0.5
F-14	68	M	IdCMP	--	--	+	--	+	--	0.1
F-15	57	F	IsCMP	--	--	+	--	+	--	0.4
F-16	70	M	IdCMP	--	--	+	+	+	--	0.5
F-17	66	M	IsCMP	--	--	--	+	+	--	0.35
F-18	60	F	DCM	--	--	--	--	--	--	0.1
F-19	32	F	IdCMP	NA	NA	NA	NA	NA	NA	0.1
F-20	56	F	IsCMP	NA	NA	NA	NA	NA	NA	0.05
F-21	53	M	DCM	--	--	+	+	+	--	0.1
F-22	57	M	IsCMP	--	--	--	--	--	--	0.35
F-23	52	M	IdCMP	--	--	+	+		--	0.1
F-24	61	M	IdCMP	--	--	--	--	+	--	0.1

MVD, mitral valve defect; VSD, ventricular septal defect; IsCMP, ischemic cardiomyopathy; DCM, dilated cardiomyopathy, IdCMP, idiopathic dilated cardiomyopathy; Dgn, digoxin, Dbt, dobutamine; β-Blk, β-adrenergic blocker, ACEI, angiotensin converting enzyme inhibitor, Ca-Blx, calcium channel blocker, NA, not available. SIRT6 levels determined by western blotting were normalized against expression of loading control (actin or tubulin) and presented as fold change over NF1.

Table 2: Primer sequences.

Primer Name	Forward Sequence (5'→ 3')	Reverse Sequence (5'→ 3')
Primer sequences used for the ChIP assay with mouse tissues or cell lines		
mAkt1ChIP1	ATTTCCATCCTGGGCGATAGC	CCAGAAGCCCGACTTGATAGTAAC
mAkt1ChIP2	GTACTGGGTTGGATGAGCCCTCAATAG	CAGCGTGGGAAGTGAATCAGTTTGAC
mAkt3ChIP1	GGAGCCATCATGAGCGATGTTAC	TTGATTCAACAGCGCCAGAGG
mAkt3ChIP2	TGCCACAAGACCAGAGCAGTGTATTC	CAATTGGCCTGACCGCACATAAAG
mMapk3ChIP1	CCGGGTGGGTTCCCTTAGCATTACTG	ACCCGGCTTTCCCGCCTAGTTAC
mMapk3ChIP2	GATGGCTCAGGCCTAAAG	AGTGGCCCTCAGTAATGC
mGsk3bChIP1	TGCCAGTGTCCACTCTAAC	TGTAGTCCAGCGTCCATTG
mGsk3bChIP2	GAACAATGGACGCTGGACTACATGTG	ATGTGGTCAGGACAGTACCTCGAATC
mIgf1rChIP1	CGTGCTCGGCTTTGACCTTC	CGCGAGCTCCTTCCCAAATCCAG
mIgf1rChIP2	TGTAGCCGCTTGGAGTGTGC	CCGCTCAGCGGAGTTAATG
mIgf2rChIP1	GTGGTGGTACACGCTTCTAAAC	GGTGACTGGTGGACTAATATGC
mIgf2rChIP2	GTTGTCAGGCCTCGAGTAG	ACGTGACGTCCTCGTTCAG
mIrs2ChIP1	TCACGCTCATTGGTCCGTCTCG	CCGCCGCACAGTGAGTAACACATC
mIrs2ChIP2	CCCTTTCCCGGCACTATGGAAACC	GGGCGTCATCAGAGCCATTCACTTG
mTorChIP1	CTCAGTGAACCGATTTCC	ACGGTTTGGTACCCTAAG
mTorChIP2	TCCCGAGCACGATCCCTAAC	CCACGAACACTTCCGGTACG
mPtenChIP1	TGTGAGGTGCACTCTATTCACGGAGAC	GGGTTCATTTGCCCGAAAGATGAACG
mPtenChIP2	ACGCGGGAGACACAATAGG	GTCGGCGACAGTCTTTAC
mTsc2ChIP1	GGGCAAGGCATAGCCTAATCG	TGGAGACCTGCCAGGAGTTC
mTsc2ChIP2	CTTGGCTCTGTTGCCAAAG	ATCCTGCAGACCGATGATG
Primers used for the ChIP assay with human cell lines		
hAKT1ChIP-1	TGCTGGCCTGGTGTATACG	CAGAGGGCTGGACTCAAAGAC
hAKT1ChIP-2	AGTTGTCGGAGGAACTTCTG	CCGGGTATGGAATGAGTAAGTG
hAKT3ChIP-1	TATTTGGGTAGGCGTGACTG	AGCACTTCCCTAGTCTTG
hAKT3ChIP-2	CTGGCGACAGAGTGAGATTCC	AAACCAGTCACGCCTACCC
hMAPK3ChIP-1	TGCCTTTCTTCAGTCCCTACCTTC	AGCTGAGATTGCACCACTTCAC
hMAPK3ChIP-2	TCGTAGTCCCAGCTCTTTG	TTCCATGCCTCTCAGAGTC
hGSK3bChIP-1	CACCAATCACCGAAGGAGGTACG	AATCAGAGTCGCCGGCCCTTACG
hGSK3bChIP-2	GCAGCTAGGTCTTGCGATTG	GGAGGGCGTCTATAAAGCG
hIGF1rChIP-1	GGAGCGAAGACTGAGTTTG	GGAGCCAGACTTCATTCC
hIGF1rChIP-2	GTTCGGGCTTTCCAGTACG	GGCTGGGAGAGGTTCATTG
hIGF2rChIP-1	CCCACGCTTGGGAAATAAC	AGTGCCAGGGAGGTAAATG
hIGF2rChIP-2	TTGACTCCACGGGCAGTTAAAG	CAAAGTGCCAGGGAGGTAAATG
hIRS2ChIP-1	CTCGGTGCGCGATGTGTTACTC	TGCTGCTGCTGCTGGTGTTG
hIRS2ChIP-2	GCGCTATGGAAACCGCACTTTCTCCG	GCGCCATTCACTTGTCAGCTTGTCG
hmTORChIP-1	TCCATAAAGAGCGCTAGCC	CTCCCGGTGTAATTCTGAGAG
hMTORChIP-2	AAGGGAATCCTAGCAGCGCCGTACC	AAGCTTCAGGACCCGGCTTCTCCAG
hPTENChIP-1	TGCAAGGGAGCCGGATGAGGTGATAC	CACCGCTGTCGGATCACAATCGTTCG

hPTENChIP-2	CTGCTCAACGCACCCATCTCAGCTTTC	AGCAACGCGAGGCGAGGATAACG
hTsc2ChIP-1	CGAGCCTGAGATGCTTGAC	CTGGGCAAGCTCATCTACC
hTsc2ChIP-2	GCCGAGGCAGGAGAATAATTTG	TAGTGATGGGCCAGATAC
Primers used for the real-time PCR analysis		
Akt1	TGGACAAGGACGGGCACATCAAG	TACTCCGGCGTTCCGCAGAATG
Akt2	TGTGGGCGACTTCATCCTTTGC	TTCGGCAAGGTCATTCTGGTTCG
Akt3	CATAGGCTATAAGGAGAAACC	TTGGATAGCTTCCGTCCAC
Insulin1	GAAGTGGAGGACCCACAAGTG	CTGAAGGTCCCCGGGGCT
Insulin2	TGCTGATGCCCTGGCCTGCTCT	CTGGTCCCACATATGCACATGCA
Gsk3β	TCCATTCCTTTGGAATCTGC	CAATTCAGCCAACACACACAGC
Irs2	CGCCGCTACAGCGAAGTACT	CGGACGCCAAGCACAAGT
FoxO1	TCGTACGCCGACCTCATCA	CTGTCGCCCTTATCCTTGAAGT
Pten	AATTCCCAGTCAGAGGCGCTATGT	GATTGCAAGTTCCGCCACTGAACA
mTor	GAGAACCAGCCCATAAGA	ACCAGCCAATGTAGCACT
Igf1	TCATGTCGTCTTCACACCTCTTCT	CCACACACGAACTGAAGAGCAT
Igf2	ACAACTTCGATTTGAACCACATTC	GAGAGCTCAAACCATGCAAACT
Igf1r	GTGGGGGCTCGTGTTTCTC	GATCACCGTGCAGTTTTCCA
Igf2r	GGGAAGCTGTTGACTCCAAAA	GCAGCCCATAGTGGTGTTGAA
Insr	ATGGGCTTCGGGAGAGGAT	GGATGTCCATACCAGGGCAC
Mapk3	AGGGCTACACCAAATCCATC	GGGAACCCAAGATACCTAGAA
Igfbp3	GAGTGTGGAAAGCCAGGTTGTC	GCATGGAGTGGATGGAACTTG
At1	GTTCCTGCTCACGTGTCTCA	CATCAGCCAGATGATGATGC
At4	GATGAAGGCACACCATCCAT	AAACCAGCCTTTCTCGGTTCT
GAPDH	ATGGTGAAGAAGGTCGGTGTGA	AATCTCCACTTTGCCACTGC
RPL32	ACAACAGGGTGCGGAGAAGATT	GTGACTCTGATGGCCAGCTGT
18S	GGACAGGATTGACAGATTGATAG	CTCGTTCGTTTATCGGAATTAAC